



# Automatic classification of normal/AD brain MRI slices using whale-algorithm optimized hybrid image features

Seifedine Kadry<sup>1,2,3,5</sup> · V. Elizabeth Jessy<sup>4,5</sup> · Venkatesan Rajinikanth<sup>4,5</sup> · Rubén González Crespo<sup>4,5</sup>

Received: 18 March 2023 / Accepted: 19 July 2023 / Published online: 29 July 2023  
© The Author(s), under exclusive licence to Springer-Verlag GmbH Germany, part of Springer Nature 2023

## Abstract

In recent years, the prevalence of Age-Related Illnesses (ARL) has been increasing among older individuals, and early recognition and treatment will result in better living conditions. It is well known that Alzheimer's Disease (AD) is among the ARD, and severe cases may result in dementia as well. It is the purpose of this study to propose a technique for distinguishing normal/AD brain MRI slices with improved accuracy utilizing the T2-modality. This scheme consists following phases: (i) Brain MRI collection and preprocessing, (ii) Deep feature extraction with the chosen scheme, (iii) Handcrafted feature extraction, (iv) Whale Algorithm (WA) based feature reduction and serial integration, and (v) binary classification using five-fold cross-validation. A total of 2000 MRI slices (1000 normal and 1000 AD class) are examined during this task using images collected from Alzheimer's Disease Neuroimaging Initiative (ADNI). This study confirms that the proposed scheme provides a classification accuracy of > 98% when applied with the K-Nearest Classifier.

**Keywords** Alzheimer's disease · Brain MRI · T2-modality · Deep-learning · Whale algorithm · Classification

## 1 Introduction

The increasing number of individuals over 60 years, as highlighted by the World Health Organization (WHO) survey on aging, has significant implications for societies worldwide. In 2019, the global population of people aged 60 and above reached 1 billion ([https://www.who.int/health-topics/ageing#tab=tab\\_1](https://www.who.int/health-topics/ageing#tab=tab_1)). The WHO projects that this number will

continue to rise, reaching 1.4 billion by 2030 and 2.1 billion by 2050 (<https://www.who.int/news-room/fact-sheets/detail/ageing-and-health>). One notable aspect emphasized by the WHO is that a significant proportion of the elderly population, approximately 80%, will reside in low- and middle-income countries by 2050. This trend emphasizes the importance of addressing the needs of older adults in these countries, as they may face additional challenges in accessing adequate healthcare and social support.

To effectively cater to the needs of older adults, governments must implement changes across various sectors, particularly in health and social care. Recognizing the growing prevalence of age-related illnesses among the elderly, early detection and assistance is crucial for minimizing their impact (Striegl et al. 2022; Alves et al. 2022; Mason et al. 2022). Efforts should focus on promoting preventive measures, providing accessible and affordable healthcare services, and developing comprehensive support systems for older adults.

Creating a healthy living environment for seniors has gained significant attention recently. This involves ensuring that older adults have access to safe and age-friendly communities, good housing options, transportation services, and social engagement opportunities. Furthermore, promoting healthy aging through lifestyle interventions,

✉ Rubén González Crespo  
ruben.gonzalez@unir.net

<sup>1</sup> Department of Applied Data Science, Noroff University College, 4612 Kristiansand, Norway

<sup>2</sup> Artificial Intelligence Research Center (AIRC), College of Engineering and Information Technology, Ajman University, Ajman, United Arab Emirates

<sup>3</sup> Department of Electrical and Computer Engineering, Lebanese American University, Byblos, Lebanon

<sup>4</sup> Division of Research and Innovation, Department of Computer Science and Engineering, Saveetha School of Engineering, SIMATS, Chennai 602105, Tamil Nadu, India

<sup>5</sup> Department of Computer Science and Technology, Universidad Internacional de La Rioja, Logroño, La Rioja, Spain

such as encouraging physical activity, nutritious diets, and mental well-being, is vital to enhancing older adults' quality of life (Striegl et al. 2022; Alves et al. 2022; Mason et al. 2022). Further, the increasing number of individuals aged over 60 years presents both challenges and opportunities for societies worldwide. Governments must recognize the changing demographics and make the necessary changes in various sectors, including health and social care, to cater to the needs of older adults. By prioritizing healthy aging and providing support systems, societies can better address the needs of older adults and enhance their well-being.

In humans, the brain is a vital internal organ, and abnormalities in the brain can lead to various physiological and psychological issues. These abnormalities can arise from heredity, accidents, infections, and aging. Brain-related problems initiated by aging are widespread among older individuals, and it is crucial to detect and address them effectively to minimize their impact. Several protocols have been developed to examine and diagnose brain abnormalities that utilize brain signals and images. By using techniques such as electroencephalography (EEG), functional magnetic resonance imaging (fMRI), and computed tomography (CT) scans, healthcare professionals can gather valuable information about brain function and structure. These examinations provide insights into the underlying causes of brain-related issues and help guide appropriate treatment and intervention strategies (Wang et al. 2018; Haaksma et al. 2017; Rajinikanth et al. 2023).

Early detection of brain abnormalities is crucial for timely intervention and management. It allows healthcare providers to develop personalized treatment plans and interventions tailored to the individual's needs. Additionally, advancements in neuroscience and medical technology continue to contribute to creating more accurate and efficient brain examination protocols, improving our understanding of brain disorders and enhancing patient care.

Recently, brain condition monitoring research has attracted scientists, and several works related to MRI analysis are executed using machine and deep learning schemes. The proposed research aims to examine Alzheimer's disease (AD) using the T2-modality axial-plane MRI slices. AD is the primary motivation of dementia in the aged, and it is caused by the death of brain cells due to aging. Approximately 5.8 million Americans over the age of 65 have Alzheimer's disease, according to a recent report. Over half a million people in the world suffer from dementia, and 70% will have Alzheimer's disease. For this reason, computerized disease examination frameworks have been developed to screen AD using MRI slices (Malik and Robertson 2017; Braskie et al. 2013).

MRI can be used to examine the cognitive ability and behavior of an aged individual. However, AD causes severe problems with thinking, memory, and other living behaviors.

As a result of this unchangeable obliteration, cerebral aptitudes are harshly damaged in the later stages of life, so special diagnostic practices are developed for early recognition of AD. Even though MRIs are effective at distinguishing AD symbols in the brain, they are time-consuming, primarily because they require manual examinations. It was demonstrated by Acharya et al. (2019) that different MLMs can be used to assess AD, using both benchmark and clinically collected brain MRI slices. According to this study, carefully selected features enhance AD detection performance, delivering 98.48% accuracy. Table 1 summarizes a few chosen AD detection methods.

Along with the above-said methods, other deep-learning schemes, such as Ramzan et al. (2019) (accuracy = 97.88%), Parmar et al. (2020) (accuracy = 93%), Puete-Castro et al. (2020) (accuracy = 78.72%) and Odusami et al. (2022) (accuracy = 98.86%) presented a better result with ADNI data. Hence, this research aims to develop an arrangement that can provide better detection accuracy compared to other existing methods in the literature. The earlier works in the literature confirms that the detection accuracy available for the ADNI database is only up to 99% and in order to improve this value further, it is necessary to implement new procedures, which integrates the deep and conventional feature extraction methods to provide a better detection.

Machine learning and deep learning techniques are used to detect brain diseases automatically based on disease-evidence-information-supported methods (Rajinikanth and Kadry 2021). To improve detection accuracy, this research integrates deep and handcrafted features. It consists of (i) data processing, (ii) deep-features mining, (iii) handcrafted feature mining with discrete-wavelet-transforms (DWT) and local-binary-patterns (LBP), (iv) Whale-algorithm feature reduction, and (v) serial features integration. The experimental investigation uses pre-trained methods, such as VGG16, VGG19, ResNet18, ResNet50, and ResNet101, and the results are compared and verified. Python® is used to implement the proposed empirical research, and similar results are compared to the literature results.

The contributions of this research include:

1. A detailed comparative analysis of pretrained deep-learning supported evaluation is presented for ADNI data,
2. Examination of AD in MRI slice is presented using DF and HF,
3. Feature optimization is executed with Whale Algorithm (WA), which helps to get a better result.

There are other parts to this work, which are divided into three sections; the second section presents the methodology, and third and fourth sections give the results and conclusions of this work.

**Table 1** Summary of chosen MRI-supported AD detection procedures

References	Methodology
Wang et al. (2018)	AD detection from MRI is presented using the recurrent neural network-assisted modeling technique
Haaksma et al. (2017)	A comprehensive review on the existing methods to find the AD is presented and discussed
Malik and Robertson (2017)	This work presents various procedures available to detect AD using MRI slices
Braskie et al. (2013)	Discussion of various assessment procedures and the invented methods to accurately detect the AD is discussed
Stonnington et al. (2010)	This research presents the development of the chemical score to identify the AD
Beheshti et al. (2017)	Successful categorization of the MRI slices into normal/AD class using ML scheme is discussed and this research employed a binary classifier to achieve a superior result
Dimitriadis et al. (2018)	Radom-forest (RF) supported categorization of the AD is presented with MRI slices
Islam and Zhang (2017)	Implementation of Inception-V4 approach with a multi-class classifier is presented and this work offered an accuracy of 73.75%
Ghazal et al. (2022)	This work proposed a transfer learning scheme by employing the AlexNet and achieved a testing accuracy of 91.70% on the chosen AD database
Zhang et al. (2017)	Detection of the AD from the chosen MRI database is executed with landmark-based features and achieved an accuracy of 79.02%
Chui et al. (2022)	This work implements GAN-CNN supported AD detection using benchmark MRI database and achieved 97.50% accuracy
Sharma et al. (2022)	Proposal of a novel deep learning scheme called ADNet is discussed to detect the AD and achieved an accuracy of 97.29%
Savaş (2022)	Implementation of EfficientNetB3 is discussed and achieved 97.28% accuracy with benchmark ADNI database
Lu et al. (2022)	A detailed assessment of AD detection is presented and achieved 94.50% accuracy with ADNI database

## 2 Methodology

The advantage of this technique depends on the phases considered to construct the scheme. In this work, the proposed methodology integrates the deep features with traditional handcrafted features and classifies the considered MRI slices using binary classifiers with fivefold cross-validation.

Figure 1 portrays the phases in the implemented scheme, which consist of image recording, 3D to 2D conversion, resizing, feature extraction and reduction, serial integration, and classification. First, the necessary 3D MRI (T2-modality) is collected from the ADNI database. Then, 3D to 2D conversion is implemented using ITK-snap, and only the axial-plane slice is considered for the assessment after resizing it to  $224 \times 224 \times 3$  pixels. Next, the feature from this imagery is extracted using the chosen method; a classification task is executed to find the classifier's performance with the SM classifier. After verifying the performance of chosen deep learning model, the handcrafted features are extracted using DWT and LBP and optimized using the Whale Algorithm (WA). The deep features (DF) and handcrafted features (HF) are then integrated serially to get a dominant feature vector, and the achieved result with the chosen classifier is validated. This work implements a fivefold cross-validation, and the result of this study confirms the clinical significance of the developed technique.

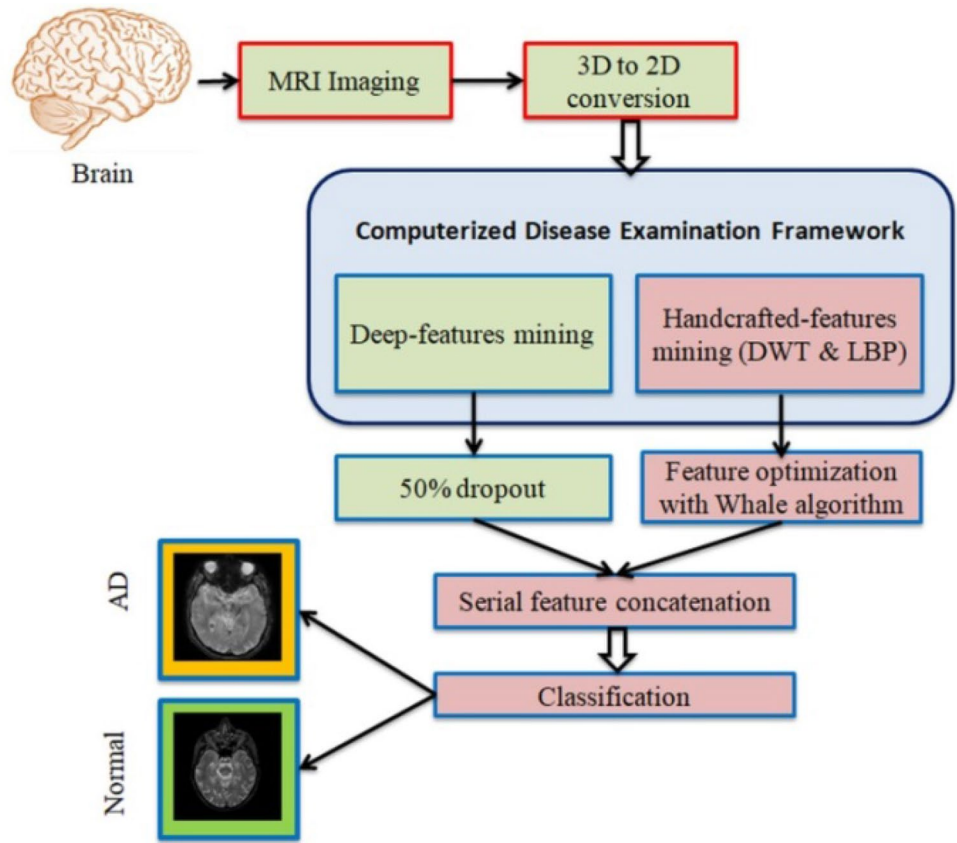
### 2.1 Image collection

For the purpose of this study, 2000 MRI slices (1000 normal and 1000 AD) are examined using the benchmark ADNI database (Petersen et al. 2010). Among these images, 80% are considered to train the system, 10% are considered to test the system, and 10% are considered to validate the performance of the proposed CDEF. Using ITK-Snap (Yushkevich et al. 2006), the collected database is converted from 3 to 2D, and the converted image is resized and analyzed. Figure 2 shows the sample test images for regular and AD classes, respectively. Images with  $224 \times 224 \times 3$  pixels are considered for this analysis, and the scheme developed doesn't apply skull stripping to the considered images.

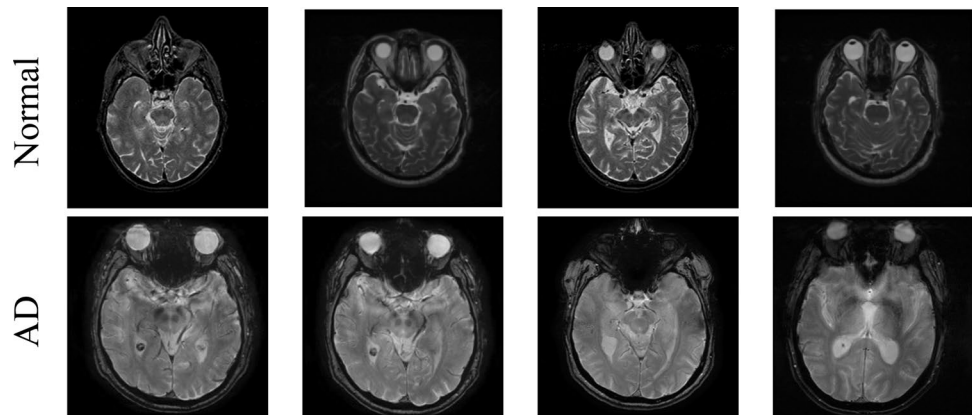
### 2.2 Feature extraction

Image features are necessary in the automatic analysis of medical data. The performance of the implemented scheme depends mainly on (i) Extracted DF with the chosen technique and (ii) extracted HF. The literature confirm that the integration of DF and HF (DF + HF) presents a better result on a class of image databases (Rajinikanth et al. 2023, 2022; Kadry et al. 2022). To achieve a better outcome from the chosen deep-learning methods, the following initial values are assigned; initial weights = ImageNet, batch value = 8, epochs = 100, optimizer = Adam, pooling = average, monitoring metric = accuracy, and loss, classifier = SoftMax with fivefold cross-validation (Khan et al. 2021).

**Fig. 1** Scheme of the proposed AD detection process



**Fig. 2** Sample MRI of normal and AD class



The DF collected are presented in Eq. (1). This feature’s 50% dropout is shown in Eq. (2);

$$DF_{(1 \times 1 \times 1000)} = DF_{(1,1)}, DF_{(1,2)}, \dots, DF_{(1,1000)} \quad (1)$$

$$DF_{50\% (1 \times 1 \times 500)} = DF_{(1,1)}, DF_{(1,2)}, \dots, DF_{(1,500)} \quad (2)$$

Later the HF is extracted using DWT and LBP, and these values are then integrated with DF after the optimization task. The DWT feature-supported AD detection is already discussed in Acharya et al. (Beheshti et al. 2017). The earlier work on DWT-enhanced images can be found in Smith

et al. (1998); Vijayakumar et al. (2022). In this work, this approach helps to get four different image cases, such as approximate, horizontal, vertical, and diagonal images, as in Fig. 3a. These images provided prime features as depicted in Eq. (3).

$$DWT_{(1 \times 1 \times 240)} = DWT_{(1,1)}, DWT_{(1,2)}, \dots, DWT_{(1,240)} \quad (3)$$

In this research, the necessary LBP features are mined as per the guidance provided by Gudigar et al. (2019). This work discusses the enhancement of the image with LBP

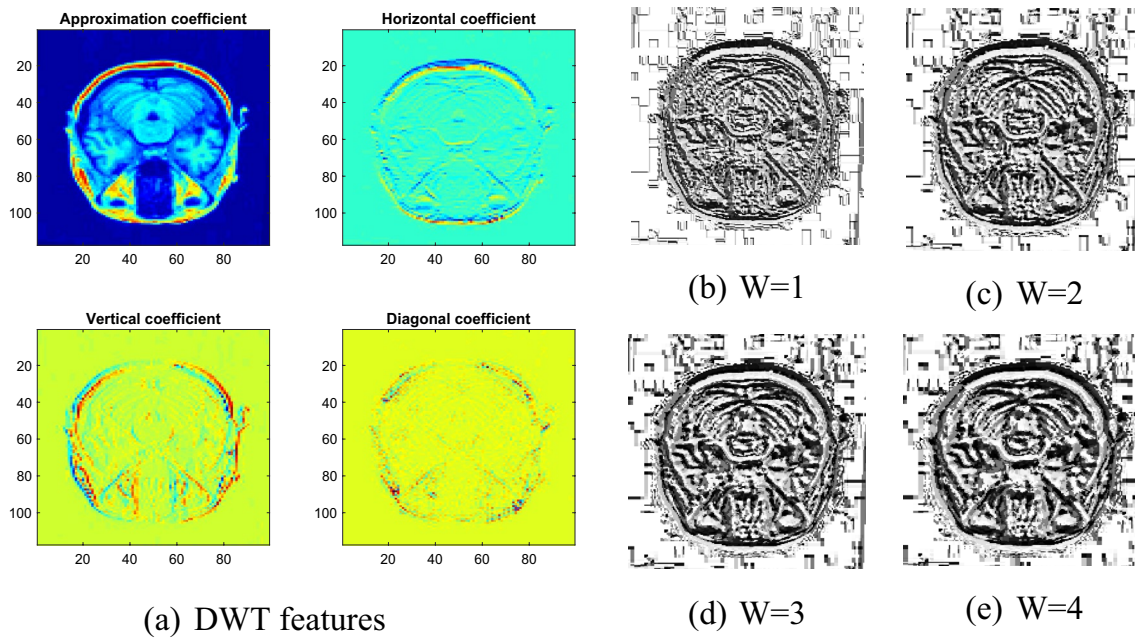


**Fig. 3** Handcrafted features of AD class MRI slice

using various weights ( $W$ ) ranging from  $W = 1$  to  $W = 4$ , and the achieved outcome for a sample image is depicted in Fig. 3b–e. From each image, 1D LBP feature vector of size  $1 \times 1 \times 59$  is extracted, and the total features will be  $59 \times 4 = 236$ .

The cumulative LBP feature obtained from the images with  $W = 1$  to  $W = 4$  is shown in Eq. (4);

$$LBP_{(1 \times 1 \times 236)} = LBP1_{(1,59)} + LBP2_{(1,59)} + LBP3_{(1,59)} + LBP4_{(1,59)} \quad (4)$$

The serial integration of Eqs. (3) and (4) presents the HF as depicted in Eq. (5) equation is optimized using the WA and these are then united with Eq. (2) to get the hybrid feature (DF + HF) vector.

$$HF_{(1 \times 1 \times 476)} = DWT_{(1 \times 1 \times 240)} + LBP_{(1 \times 1 \times 236)} \quad (5)$$

### 2.3 Feature optimization using Whale algorithm

The earlier disease detection schemes with MLM and DLM confirm the need for a feature selection/reduction procedure to avoid the over-fitting problem. The traditional feature selection methods (Student's t-test) employ a chosen mathematical scheme to reduce the feature vector (Sree et al. 2021; Oh et al. 2021; Sridhar et al. 2021). On the other hand, Heuristic Algorithm (HA) based feature optimization is widely employed by researchers to reduce the feature vector dimension. A number of recent methods employ various approaches for restore reduction and automatic disease examination (Jayachitra and Prasanth 2021;

Sekar et al. 2022; Balasubramaniam et al. 2022). In this scheme, the features of standard and disease classes are compared, and the feature which shows a significant dissimilarity will be selected. Earlier research on HA-based feature optimization can be found in Vijayakumar et al. (2022). The earlier works in the literature shows that the Whale Algorithm (WA) provides a better feature selection on the brain MRI dataset based AD detection (Dhakhina-moorthy et al. 2023). Hence, this work employed the WA to select the HF.

WA is a successful HA, invented by Mirjalili and Lewis (2016), and this algorithm mimics the foraging and hunting tactics followed by humpback whales. The traditional WA consists of the following operations: searching prey, encircling prey, bubble-net formation, and hunting. This work considered the traditional WA with the parameters discussed in Aljarah et al. (2018), and the necessary mathematical expressions and their values can be found in Mirjalili et al. (2020); Abdel-Basset et al. 2018; Mafarja and Mirjalili 2018).

The stages of the WA can be expressed as;

Step 1: Initialize the population: Create an initial population of potential solutions (whales) denoted by  $X_i$ , where  $i = 1$  to  $N$ , and  $N$  is the population size.

Step 2: Define the fitness function: Define a fitness function that evaluates the quality of each whale. The fitness function is typically denoted as  $f(X_i)$ , where  $X_i$  represents the position of the  $i$ th whale.

Step 3: Set algorithm parameters

Step 4: Update positions and encodings: Calculate the updated position of each whale using the following equation:  $X_i(t+1) = X_i(t) - A_i D_i$ , where  $t$  is the current iteration,  $A_i$  is the vector of random values in  $[0, 1]$ , and  $D_i$  represents the distance between the current position and the leader position. Apply a search operator to maintain the position within the defined search space boundaries if necessary.

Step 5: Update fitness values: Evaluate the fitness of each updated whale by calculating  $f(X_i(t+1))$ .

Step 6: Bubble-net feeding behavior: Calculate the updated position of each whale using the following equation:  $X_i(t+1) = X_i(t) - A_i D_i$ , where  $A_i$  is a random vector in  $[-1, 1]$ .

Step 7: Breaching behavior: Calculate the updated position of each whale using the following equation:  $X_i(t+1) = X_1 - A_i |C_1 X_i(t) - X_1|$ , where  $X_1$  represents the position of the leader whale,  $X_1$  denotes the target position, and  $C_1$  is a random value in  $[0, 1]$ . Calculate the updated position of each whale using the following equation:  $X_i(t+1) = X(t) - A_i (E_i |X(t) - X_c|)$ , where  $X_c$  represents the position of a random whale other than the current whale,  $E_i$  is a random value in  $[0, 1]$ , and  $A_i$  is a random vector in  $[-1, 1]$ .

Step 8: Update the leader whale: Determine the whale with the best fitness value (leader whale) in the current population. Update the leader whale's position using the following equation:  $X_1 = X_1 - A_1 |C_1 X_1 - X_1|$ , where  $A_1$  is a random value in  $[0, 2]$  and  $C_1$  is a random value in  $[-1, 1]$ . Update other whales: Update the positions of the remaining whales using the following equation:  $X_i(t+1) = X_i - A_i |C_1 X_i(t) - X_i|$ , where  $A_i$  and  $C_1$  are as defined above.

Step 9: Check termination criteria: Check if the termination criteria are met, such as reaching the maximum number of iterations or achieving a desired fitness level.

This work assigns the following parameters for the WA; agent dimension = 30, iteration value ( $Iter_{max}$ ) = 3000, termination condition =  $Iter_{max}$ . The traditional WA working is depicted in Fig. 4a, and the corresponding mathematical expressions are presented below;

The essential information regarding WA and its feature selection method can be accessed from Hussien et al. (2019); Hu et al. 2022; Murugesan et al. 2021). Figure 4b demonstrates the WA-based selection of the features from the features collected from standard/AD class images. Every feature is individually compared with each other, and the feature which demonstrates a significant difference alone is selected.

The proposed scheme reduces the HF from a value of  $1 \times 1 \times 476$  to  $1 \times 1 \times 192$  features and the reduced value is then serially integrated with the DF to acquire a new feature vector (DF+HF) with a dimension  $1 \times 1 \times 692$ , which is used to authenticate the AD detection performance of employed CDEF. The final feature vector considered to verify the performance of the classifier is presented in Eq. (6).

$$DF + HF_{(1 \times 1 \times 692)} = DF_{(1 \times 1 \times 500)} + HF_{(1 \times 1 \times 192)} \quad (6)$$

## 2.4 Performance evaluation

Using binary classification schemes with DF and DF+HF, the proposed CDEF's AD detection performance is evaluated, and the necessary metrics, including True-Positive (TP), True-Negative (TN), False-Positive (FP), and

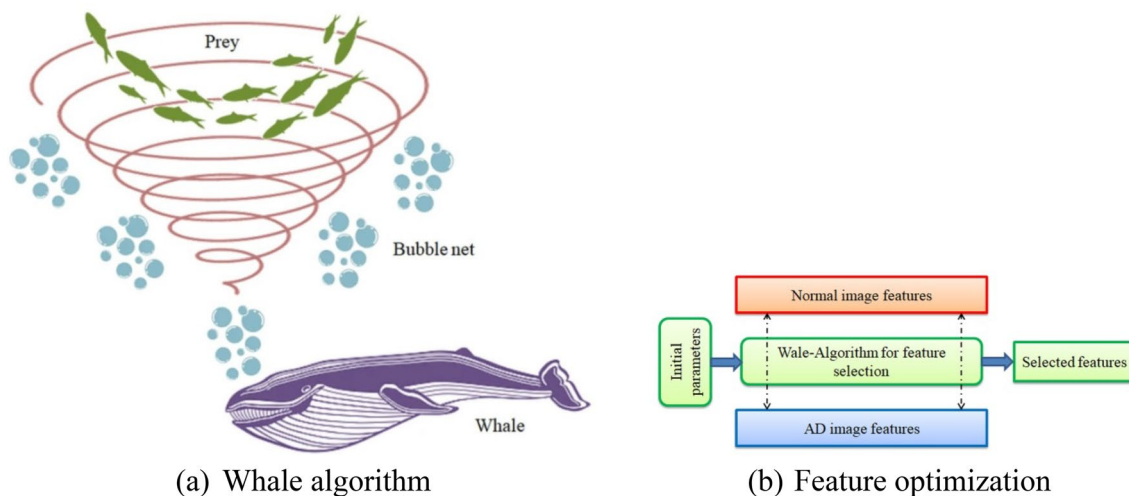


Fig. 4 Working scheme of whale algorithm

False-Negative (FN), are computed. These values are then used to derive other essential measures, such as accuracy (AC), precision (PR), sensitivity (SE), specificity (SP), and F1 Score (FS) (Roy and Singh 2023). These measures are expressed in Eqs. (7) to (11). In this work, binary classifiers such as SoftMax, Decision-Tree, K-Nearest Neighbor, Random-Forest, and Support-Vector-Machine with linear kernel are considered, and additional information can be found in Singh and Jain (2023); Rajinikanth et al. 2021).

$$AC = \frac{TP + TN}{TP + TN + FP + FN} \quad (7)$$

$$PR = \frac{TP}{TP + FP} \quad (8)$$

$$SE = \frac{TP}{TP + FN} \quad (9)$$

$$SP = \frac{TN}{TN + FP} \quad (10)$$

$$F1S = \frac{2TP}{2TP + FN + FP} \quad (11)$$

### 3 Result and discussions

As part of the research, the developed scheme considers the VGG16 model with an Intel i5 processor and 16 GB RAM working with Python<sup>®</sup>. A fivefold cross-validation scheme is used to verify the merit of the proposed scheme against methods like VGG19, ResNet18, ResNet50, and ResNet101. The model is initially trained with 80% of the image dataset, tested with 10%, and validated with 10% of the database. Various PDAs are used to verify the performance of the default classifier (SM).

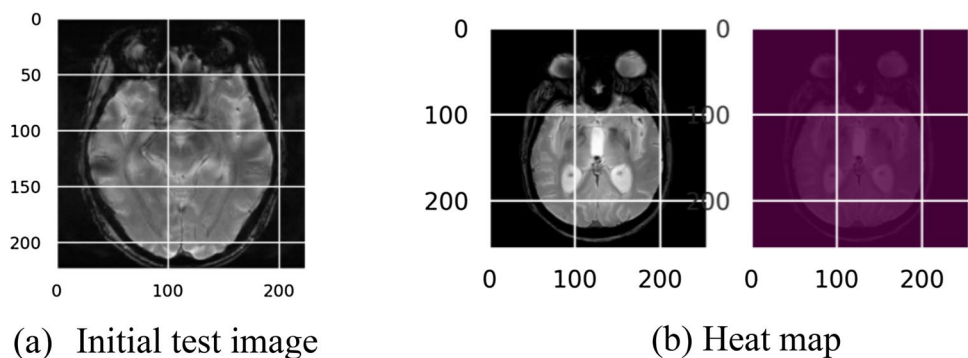
Figure 5 depicts the initial outcome achieved using the considered brain MRI slices. Figure 5a shows a sample test

image, and Fig. 5b presents the sample image along with the heat map. The outcomes of various convolution layers are then presented to demonstrate the result of the considered DLM, as in Fig. 6. Figure 6a–d demonstrates the convolution results of the pre-trained VGG16 scheme. Finally, this scheme provides a feature vector of dimension, which is then considered to classify the database into healthy/AD class after a 50% feature dropout. The results achieved in this technique are presented in Fig. 7. Figure 7a shows accuracy, and Fig. 7b illustrates the loss for chosen epochs of 100. Figure 7c and d present the confusion matrix (CM) and area under curve (AUC). Figure 9c) presents the CM achieved with TP, TN, FP, and FN values. Based on these initial values, the other metrics, like AC, PR, SE, SP, and FS, are computed as presented in Table 2.

Figure 8 presents the classification result achieved with 10% validation data, and the attained outcome confirms that the presented scheme helps to get an accuracy of > 98% when a fivefold cross-validation is employed. This procedure is repeated with other PDLA, and the results are recorded in Table 3. This confirms that the classification result achieved for VGG16 is more, and the DF-based detection provides only 96% accuracy with the RF classifier, which is lesser than the recent result by Acharya et al. (Beheshti et al. 2017). Hence, the classification task is repeated using DF + HF, and the achieved results are compared and verified. Table 3 presents the obtained result with VGG16, DF + HF, and various classifiers.

The result of Table 3 confirms the merit of VGG16 compared to other schemes. Hence, the VGG16 is considered in the developed scheme, and its performance is verified with other binary classifiers. The result achieved with the VGG16-based method for DF and DF + HF is shown in Table 3. Its graphical comparison is shown in Fig. 9. Figure 9a shows the Glyph-plot1 for the performance values achieved using the DF, Fig. 9b and c shows the Glyph-plot2 and 3 for the results achieved with HF and DF + HF, respectively. Figure 9a confirms that the RF classifier performed better than other classifiers with DF, and Fig. 9b confirms the merit of DT compared to the alternatives.

**Fig. 5** Evaluation of test picture using the proposed CDEF



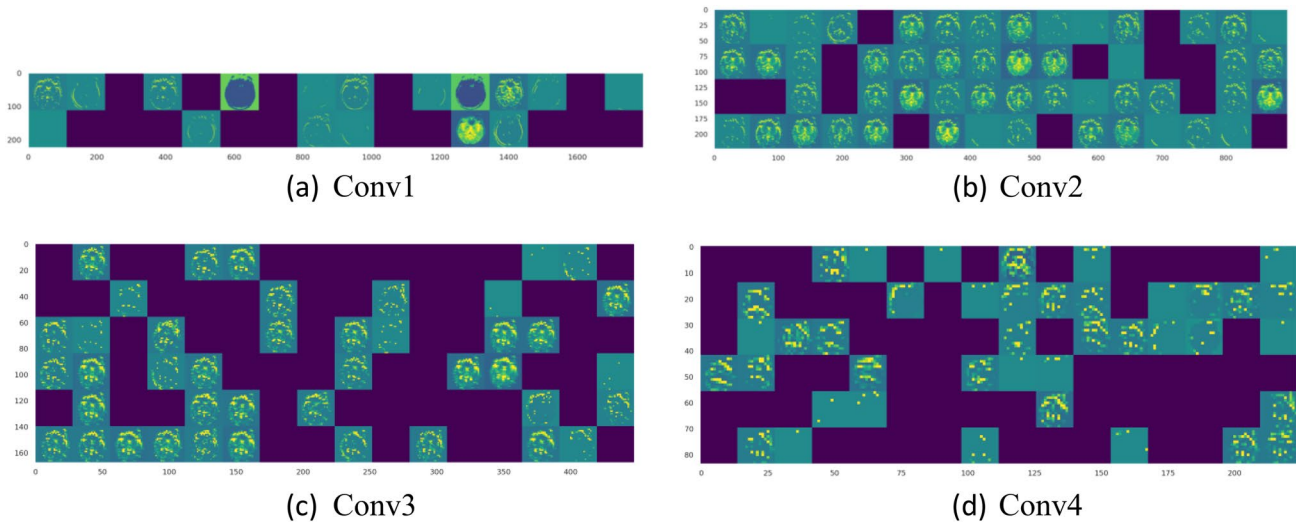


Fig. 6 Different convolution layer result during DF mining

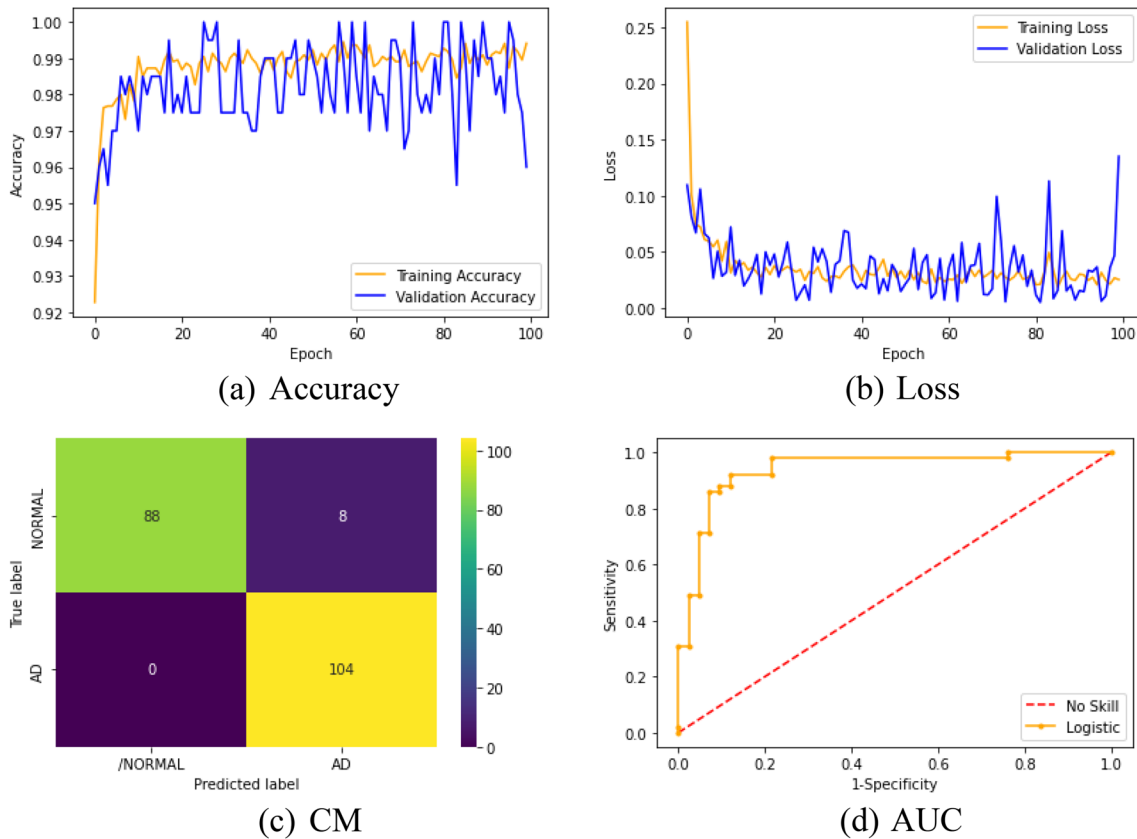


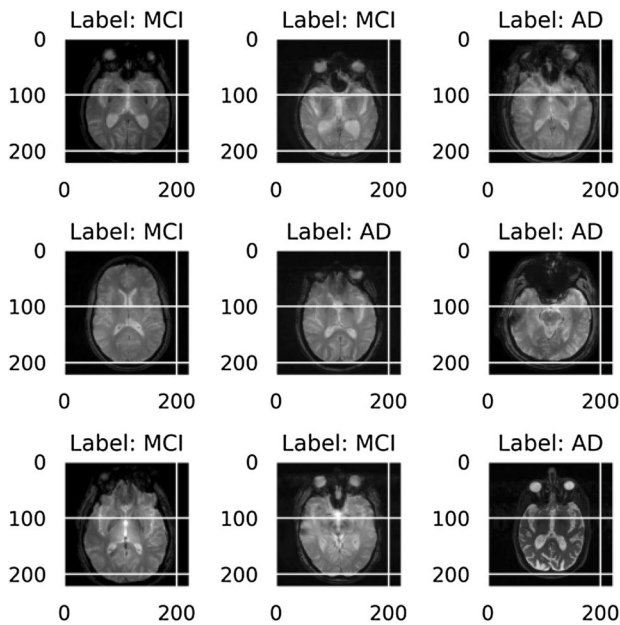
Fig. 7 Experimental outcome achieved using VGG16 with SoftMax

To verify the merit of the proposed technique, a comparative analysis with the recently developed procedures is performed, and the achieved result is presented in Fig. 10. The AD detection accuracy of the proposed method outperforms

the best results by Ghazal et al. (2022); Zhang et al. (2017); Chui et al. (2022) and is closer to the result presented in Sharma et al. (2022). This comparison confirms that this technique helps provide a result closer to the accuracy of

**Table 2** Classification results achieved with PDLA with SoftMax

CNN scheme	TP	FN	TN	FP	AC%	PR%	SE%	SP%	FS%
VGG16	84	12	98	6	91.0000	93.3333	87.5000	94.2308	90.3226
VGG19	90	8	91	11	90.5000	89.1089	91.8367	89.2157	90.4523
ResNet18	87	13	92	8	89.5000	91.5789	87.0000	92.0000	89.2308
ResNet50	92	9	89	10	90.5000	90.1961	91.0891	89.8990	90.6404
ResNet101	90	8	91	11	90.5000	89.1089	91.8367	89.2157	90.4523

**Fig. 8** Result obtained using 10% validation images

Odusami et al. (2022), which considered the fused dual deep features obtained using ResNet18 and DenseNet121 (Sharma et al. 2022). The number of optimal features in the

proposed DF + HF is considerably less compared to the work discussed in Sharma et al. (2022) and hence, the proposed AD detection technique is simple to execute compared to other earlier works presented in the literature.

## 4 Conclusion

To improve AD detection accuracy, a brain MRI examination procedure is proposed. To investigate the proposed scheme, T2-weighted axial-plane brain MRI slices of ADNI are used. DF and HF are combined in this scheme, and features are optimized using WA to achieve better detection accuracy. To identify the most appropriate pre-trained model for the selected database, (i) DF and SoftMax-based classification of the MRI slices, (ii) DF and different classifier-based classification of the MRI slices, and (iii) Normal/AD image detection. The proposed AD detection scheme achieves 96.00% detection accuracy for RF classifiers with DF and 98.50% accuracy for DT classifiers with DF + HF. As a result, this scheme has been compared and confirmed with other similar results found in the literature. This scheme can be used to detect AD in clinical MRI slices in the future.

**Table 3** Classification of MRI into normal.AD using DF and DF + HF

Features	Classifier	TP	FN	TN	FP	AC%	PR%	SE%	SP%	FS%
DF	SM	84	12	98	6	91.0000	93.3333	87.5000	94.2308	90.3226
	DT	89	10	96	5	92.5000	94.6809	89.8990	95.0495	92.2280
	KNN	91	6	96	7	93.5000	92.8571	93.8144	93.2039	93.3333
	RF	88	8	104	0	96.0000	100	91.6667	100	95.6522
	SVM	98	6	92	4	95.0000	96.0784	94.2308	95.8333	95.1456
HF	SM	84	15	82	19	83.0000	81.5534	84.8485	81.1881	83.1683
	DT	84	18	84	16	84.0000	85.7143	82.3529	85.7143	84.0000
	KNN	85	16	87	12	86.0000	87.6289	84.1584	87.8788	85.8586
	RF	83	17	85	15	84.0000	84.6939	83.0000	85.0000	83.8384
	SVM	84	15	87	14	85.5000	85.7143	84.8485	86.1386	85.2792
DF + HF	SM	97	3	97	3	97.0000	97.0000	97.0000	97.0000	97.0000
	DT	98	1	99	2	98.5000	98.0000	98.9899	98.0198	98.4925
	KNN	98	0	97	5	97.5000	95.1456	100	95.0980	97.5124
	RF	97	2	97	4	97.0000	96.0396	97.9798	96.0396	97.0000
	SVM	98	1	97	4	97.5000	96.0784	98.9899	96.0396	97.5124

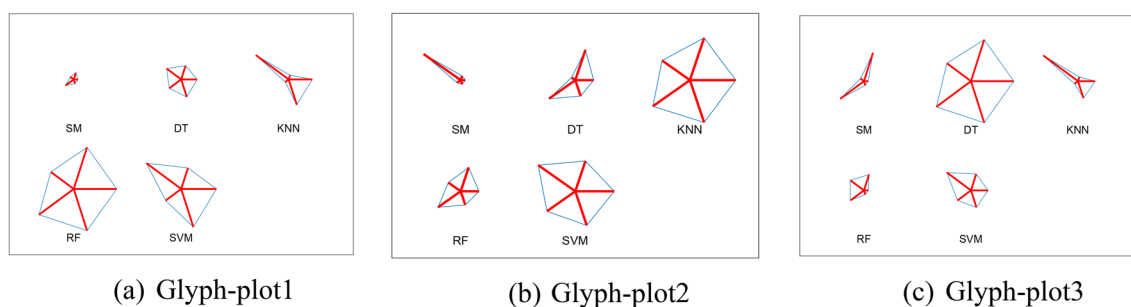
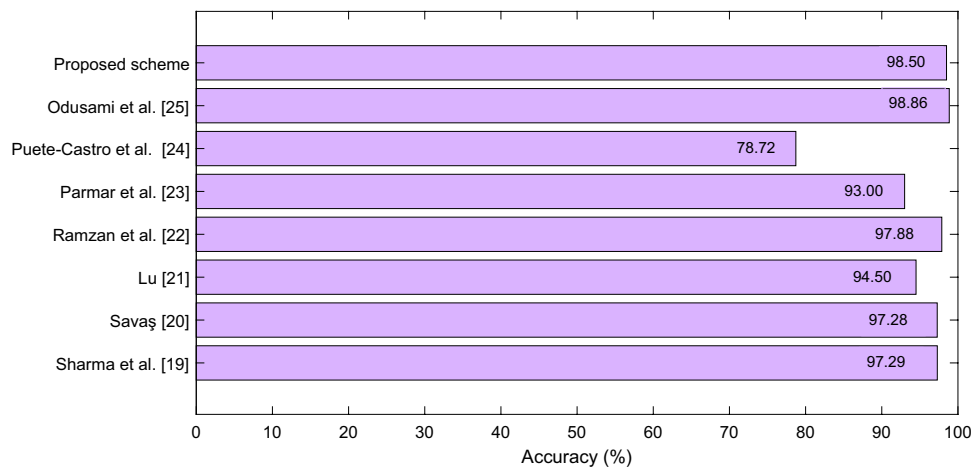


**Fig. 9** Comparison of the performance of classification result

**Fig. 10** Validation of the proposed scheme with recent literature



## Declarations

**Conflict of interest** The authors declare that they have no conflicts of interest to report regarding the present study.

## References

- Abdel-Basset M, Manogaran G, El-Shahat D, Mirjalili S (2018) Integrating the whale algorithm with tabu search for quadratic assignment problem: a new approach for locating hospital departments. *Appl Soft Comput* 73:530–546
- Acharya UR, Fernandes SL, WeiKoh JE, Ciaccio EJ et al (2019) Automated detection of Alzheimer's disease using brain MRI images—a study with various feature extraction techniques. *J Med Syst* 43(9):1–14
- Aljarah I, Faris H, Mirjalili S (2018) Optimizing connection weights in neural networks using the whale optimization algorithm. *Soft Comput* 22(1):1–15
- Alves GS, Kumar S, Sudo FK (2022) The interplay between long-term psychiatric disorders and age-related brain changes. *Front Psychiatry*. <https://doi.org/10.3389/fpsy.2022.898023>
- Balasubramaniam S, Satheesh Kumar K, Kavitha V, Prasanth A, Sivakumar TA (2022) Feature selection and dwarf mongoose optimization enabled deep learning for heart disease detection. *Comput Intell Neurosci*. <https://doi.org/10.1155/2022/2819378>
- Beheshti I, Demirel H, Matsuda H (2017) Classification of Alzheimer's disease and prediction of mild cognitive impairment-to-Alzheimer's conversion from structural magnetic resource imaging using feature ranking and a genetic algorithm. *Comput Biol Med* 83:109–119
- Braskie MN, Toga AW, Thompson PM (2013) Recent advances in imaging alzheimer's disease. *J Alzheimers Dis* 33(1):S313–S327
- Chui KT, Gupta BB, Alhalabi W, Alzahrani FS (2022) An MRI scans-based Alzheimer's disease detection via convolutional neural network and transfer learning. *Diagnostics* 12(7):1531
- Dhakhnamoorthy C, Mani SK, Mathivanan SK, Mohan S, Jayagopal P, Mallik S, Qin H (2023) Hybrid whale and gray wolf deep learning optimization algorithm for prediction of Alzheimer's disease. *Mathematics* 11(5):1136
- Dimitriadis SI, Liparas D, Tsolaki MN (2018) Random Forest feature selection, fusion and ensemble strategy: Combining multiple morphological MRI measures to discriminate among healthy elderly, MCI, cMCI and alzheimer's disease patients: From the alzheimer's disease neuroimaging initiative (ADNI) database. *J Neurosci Methods* 302:14–23
- Ghazal TM, Abbas S, Munir SA, Khan M, Ahmad M, Issa G, Binish Zahra S, Adnan Khan M, Kamrul Hasan M (2022) Alzheimer disease detection empowered with transfer learning. *Comput Mater Contin* 70(3):5005–5019
- Gudigar A, Raghavendra U, Devasia T, Nayak K, Danish SM et al (2019) Global weighted LBP based entropy features for the assessment of pulmonary hypertension. *Pattern Recognit Lett* 125:35–41
- Haaksmala ML, Vilela LR, Marengoni A, Calderón-Larrañaga A, Leoutsakos JS et al (2017) Comorbidity and progression of late onset Alzheimer's disease: a systematic review. *PLoS ONE* 12(5):e0177044

- Hu F, Zhou M, Li M, Bian K (2022) Joint feature selection of power load in time domain and frequency domain based on whale optimization algorithm. *Int Trans Electr Energy Syst*. <https://doi.org/10.1155/2022/4139379>
- Hussien AG, Hassanien AE, Houssein EH, Bhattacharyya S, Amin M (2019) S-shaped binary whale optimization algorithm for feature selection. *Recent trends in signal and image processing*. Springer, Singapore, pp 79–87
- Islam J, Zhang Y (2017) A novel deep learning based multi-class classification method for Alzheimer's disease detection using brain MRI data. In: *Brain informatics: international conference, BI 2017, Beijing, China, November 16–18, 2017, Proceedings*. Springer International Publishing, pp 213–222
- Jayachitra S, Prasanth A (2021) Multi-feature analysis for automated brain stroke classification using weighted Gaussian naïve Bayes classifier. *J Circuits Syst Comput* 30(10):2150178
- Kadry S, Rajinikanth V, González Crespo R, Verdú E (2022) Automated detection of age-related macular degeneration using a pre-trained deep-learning scheme. *J Supercomput* 78(5):7321–7340
- Khan MA, Rajinikanth V, Satapathy SC, Taniar D, Mohanty JR et al (2021) VGG19 network assisted joint segmentation and classification of lung nodules in CT images. *Diagnostics* 11(12):2208
- Lu B, Li HX, Chang ZK, Li L, Chen NX, Zhu ZC et al (2022) A practical Alzheimer's disease classifier via brain imaging-based deep learning on 85,721 samples. *J Big Data* 9(1):1–22
- Mafarja M, Mirjalili S (2018) Whale optimization approaches for wrapper feature selection. *Appl Soft Comput* 62:441–453
- Malik GA, Robertson NP (2017) Treatments in Alzheimer's disease. *J Neurol* 264(2):416–418
- Mason LM, Clarke AR, Barry RJ (2022) Age-related changes in the EEG in an eyes-open condition: II. Subtypes of AD/HD. *Int J Psychophysiol* 174:83–91
- Mirjalili S, Lewis A (2016) The whale optimization algorithm. *Adv Eng Softw* 95:51–67
- Mirjalili S, Mirjalili SM, Saremi S, Mirjalili S (2020) Whale optimization algorithm: theory, literature review, and application in designing photonic crystal filters. *Nature-inspired optimizers*. Springer, Cham, pp 219–238
- Murugesan S, Bhuvaneswaran RS, Nehemiah HK, Sankari SK, Jane YN (2021) Feature selection and classification of clinical datasets using bioinspired algorithms and super learner. *Comput Math Methods Med*. <https://doi.org/10.1155/2021/6662420>
- Odusami M, Maskeliūnas R, Damaševičius R (2022) An intelligent system for early recognition of Alzheimer's disease using neuroimaging. *Sensors* 22(3):740
- Oh SL, Jahmunah V, Arunkumar N, Abdulhay EW, Gururajan R et al (2021) A novel automated autism spectrum disorder detection system. *Complex Intell Syst* 7(5):2399–2413
- Parmar H, Nutter B, Long L, Antani S, Mitra S (2020) Spatiotemporal feature extraction and classification of Alzheimer's disease using deep learning 3D-CNN for fMRI data. *J Med Imaging* 7:056001
- Petersen RC, Aisen PS, Beckett LA, Donohue MC, Gamst AC et al (2010) Alzheimer's disease neuroimaging initiative (ADNI): clinical characterization. *Neurology* 74(3):201–209
- Puente-Castro A, Fernandez-Blanco E, Pazos A, Munteanu CR (2020) Automatic assessment of Alzheimer's disease diagnosis based on deep learning techniques. *Comput Biol Med* 120:103764
- Rajinikanth V, Kadry S (2021) Development of a framework for preserving the disease-evidence-information to support efficient disease diagnosis. *Int J Data Warehous Min (IJDWM)* 17(2):63–84
- Rajinikanth V, Aslam SM, Kadry S (2021) Deep learning framework to detect ischemic stroke lesion in brain MRI slices of flair/DW/T1 modalities. *Symmetry* 13(11):2080
- Rajinikanth V, Kadry S, Taniar D, Kamalanand K, Elaziz MA et al (2022) Detecting epilepsy in EEG signals using synchro-extracting-transform (SET) supported classification technique. *J Ambient Intell Human Comput*. <https://doi.org/10.1007/s12652-021-03676-x>
- Rajinikanth V, Kadry S, Moreno-Ger P (2023) ResNet18 supported inspection of tuberculosis in chest radiographs with integrated deep, LBP, and DWT features. *Int J Interact Multimedia Artif Intell* 8(Regular Issue, 2):38–46. <https://doi.org/10.9781/ijimai.2023.05.004>
- Ramzan F, Khan MUG, Rehmat A, Iqbal S, Saba T et al (2019) A deep learning approach for automated diagnosis and multi-class classification of Alzheimer's disease stages using resting-state fmri and residual neural networks. *J Med Syst* 44:37
- Roy PK, Singh A (2023) COVID-19 disease prediction using weighted ensemble transfer learning. *Int J Interact Multimedia Artif Intell* 8(1):13–22. <https://doi.org/10.9781/ijimai.2023.02.006>. **(Special issue on AI-driven algorithms and applications in the dynamic and evolving environments)**
- Savaş S (2022) Detecting the stages of Alzheimer's disease with pre-trained deep learning architectures. *Arab J Sci Eng* 47(2):2201–2218
- Sekar J, Aruchamy P, Sulaima Lebbe Abdul H, Mohammed AS, Khamuruddeen S (2022) An efficient clinical support system for heart disease prediction using TANFIS classifier. *Comput Intell* 38(2):610–640
- Sharma R, Goel T, Tanveer M, Murugan R (2022) FDN-ADNet: fuzzy LS-TWSVM based deep learning network for prognosis of the Alzheimer's disease using the sagittal plane of MRI scans. *Appl Soft Comput* 115:108099
- Singh V, Jain D (2023) A hybrid parallel classification model for the diagnosis of chronic kidney disease. *Int J Interact Multimedia Artif Intell* 8(Regular Issue, 2):14–28. <https://doi.org/10.9781/ijimai.2021.10.008>
- Smith LC, Turcotte DL, Isacks BL (1998) Stream flow characterization and feature detection using a discrete wavelet transform. *Hydrol Process* 12(2):233–249
- Sree V, Mapes J, Dua S, Lih OS, Koh JE et al (2021) A novel machine learning framework for automated detection of arrhythmias in ECG segments. *J Ambient Intell Humaniz Comput* 12(11):10145–10162
- Sridhar C, Lih OS, Jahmunah V, Koh JE, Ciaccio E et al (2021) Accurate detection of myocardial infarction using nonlinear features with ECG signals. *J Ambient Intell Humaniz Comput* 12(3):3227–3244
- Stonnington CM, Chu C, Klöppel S, Jack CR, Ashburner J et al (2010) Predicting clinical scores from magnetic resonance scans in Alzheimer's disease. *Neuroimage* 5(4):1405–1413
- Striegl J, Gotthardt M, Loitsch C, Weber G (2022) Investigating the usability of voice assistant-based CBT for age-related depression. *International conference on computers helping people with special needs*. Springer, Cham, pp 432–441
- Vijayakumar K, Rajinikanth V, Kirubakaran MK (2022) Automatic detection of breast cancer in ultrasound images using Mayfly algorithm optimized handcrafted features. *J X-Ray Sci Technol* 30:751–766
- Wang T, Qiu RG, Yu M (2018) Predictive modeling of the progression of Alzheimer's disease with recurrent neural networks. *Sci Rep* 8:9161
- Yushkevich PA, Piven J, Hazlett HC, Smith RG, Ho S et al (2006) User-guided 3D active contour segmentation of anatomical structures: significantly improved efficiency and reliability. *Neuroimage* 31(3):1116–1128

Zhang J, Liu M, An L, Gao Y, Shen D (2017) Alzheimer's disease diagnosis using landmark-based features from longitudinal structural MR images. *IEEE J Biomed Health Inform* 21(6):1607–1616

**Publisher's Note** Springer Nature remains neutral with regard to jurisdictional claims in published maps and institutional affiliations.

Springer Nature or its licensor (e.g. a society or other partner) holds exclusive rights to this article under a publishing agreement with the author(s) or other rightsholder(s); author self-archiving of the accepted manuscript version of this article is solely governed by the terms of such publishing agreement and applicable law.